Automation in Construction 70 (2016) 167–177

Contents lists available at ScienceDirect

Automation in Construction

journal homepage: www.elsevier.com/locate/autcon

Optimal construction site layout based on risk spatial variability

M. Abune'meh [a,b,c], R. El Meouche [a,*], I. Hijaze [b], A. Mebarki [c], I. Shahrour [d]

[a] Université Paris-Est, Institut de Recherche en Constructibilité, ESTP, F-94230 Cachan, France
[b] An-Najah National University, Urban Planning Engineering Department, P.O. Box:7, West Bank, Palestine
[c] University Paris-Est, Lab. Modélisation et Simulation Multi Echelle (MSME/UMR 8208 CNRS), 5 Bd Descartes, 77454 Marne-La-Vallée, France
[d] Laboratoire de Génie Civil et géo-Environnement, Université Lille1, 59 650 Villeneuve d'Ascq, France

ARTICLE INFO

Article history:
Received 17 July 2015
Received in revised form 26 April 2016
Accepted 22 June 2016
Available online 14 July 2016

Keywords:
Construction management
Risk
Optimization
GIS
Space syntax

ABSTRACT

The construction site layout planning is a complex and important task conducted by project managers and planners. It must able to face the occurrence of potential hazards like fire and blast waves, for instance. However, minimizing risk resulting from natural or technological hazards is still a scientific challenge.

In the present paper, a new methodology is developed in order to evaluate the risks within a construction site. It consists of:

Modeling construction site components, for instance; electric generator, fuel storage, offices, equipment and material storages, in 2D layout. These components act as hazardous sources and potential targets at the same time,

Modeling hazard interaction matrix: it shows the hazard interaction among site components and the attenuation of hazard with distance,

Modeling vulnerability interaction matrix: it represents the potential weakness of whole targets to the hazard generated from each source. In the present research, the vulnerability is expressed as function of hazard intensity,

Defining the utility function: it aims to afford an optimized site layout with minimum total risk in the construction site, finally

Performing spatial analysis technique, utilizing space syntax principle, to realize space configurations in the construction site. As the evacuation process is considered in evaluating and visualizing the risk, the actual risk is amplified by utilizing penalty factor called mean depth.

Geographic information system (GIS) is useful in visualizing the spatial variability of the risk within the site. It integrates the potential total impact of the facilities with the space configuration mean depth results. For illustration purposes, the methodology is employed in a case study consisting of several facilities acting as hazardous sources and potential targets in a 2D layout. The risk optimization considers the level of hazards at each source object, hazard attenuation and adopts conditional values for the vulnerability of the target objects. A differential evolution algorithm is adopted to minimize the global risk within the site. The results showed that the proposed methodology is efficient, due to its capability of generating site layout with safer work environment. This in turn leads to minimize work accidents, serious injuries and victims. In addition, the model is capable of highlighting the highest risk areas within a construction site.

1. Introduction

The occurrence of accidental events such as fire, blast waves and leakage of hazardous material is one main feature of the construction industry. Construction managers always aim to keep their expected consequences to a minimum level. Therefore, it is very important to adequately organize the sites in order to diminish the consequences of these hazards and provide safe work environment.

[1] stated that construction site space is one of project resources that requires management, like any other resource. In fact, the usual strategies for managing site spaces are based on the principle of “first come first served”. [2] confirmed that site layout planning is unique for each construction project and depends on work areas and locations of different facilities.

* Corresponding author.
E-mail address: relmeouche@estp-paris.eu (R. El Meouche).

http://dx.doi.org/10.1016/j.autcon.2016.06.014
0926-5805/

Site layout planning can be defined as the accommodation of supporting temporary facilities, such as electric generator, fuel storage, offices and so on, at a suitable location within the available site space. According to [3], an efficient site layout provides superior working environments quality and safe operation for labor construction. Therefore, to consider a site layout plan as efficient, it is essential to benefit from the work areas provided to minimize hazard impact and mitigate the consequences of cascading (domino) effects.

Unfortunately, construction projects are not exempt from exposure to the occurrence of natural hazards that may lead to catastrophic consequences. [29,30] indicated that fire hazard is one kind of accidents that may occur at construction sites that may lead to construction schedule disturbance. [32] found that about 4800 construction site fires occur every year, resulting in more than $ 35 million losses in property. [31] indicated that due to rapid development in the construction industries, the fire hazard is frequently occurring at construction sites.

The current site layout planning models focus entirely on reducing the travel cost distance between facilities [4]. They overlooked the potential hazards that may lead to infeasible or non-effectual solutions. In addition to this, the parties involved in construction tend to make decisions based on their own experience. Sometimes these decisions may be incomplete and/or incorrect, which in turn leads to unsafe site layouts.

However, only a few efforts have been devoted to organizing site layout for avoiding, or at least minimizing, risk of potential hazards. [4,5] developed an optimization site layout model which aims to maximize construction safety. However, these models did not take into account the potential hazards such as fire and blast waves during optimization as they rather focus on the facilities containing hazardous materials.

Therefore, it is important to properly manage a site in order to maintain the integrity of the construction site and facilitate the evacuation process during emergency cases. Evacuation is highly significant in construction site safety planning. If any hazard occurs within a site, the workers need to be evacuated safely, through crossing areas with least risk, to minimize casualties. In the current paper, the evacuation is based on integration or segregation of each position with respect to others within the site. Relevant penalty factors are actually adopted in order to generate spatial risk map.

This research aims to enhance site layout planning by developing new models that take into account the hazard and vulnerability interactions among facilities. Furthermore, after obtaining the optimal layout of facilities, the spatial analysis technique called space syntax is utilized to analyze the influence of space configurations on spatial variability of risk within a construction site.

2. Literature review

Several studies have been conducted for construction site layout planning. There is a consensus from most researchers that site layout planning is still a challenging task [2,5,6]. [2] stated that optimizing the cost, safety and productivity of a project relies on adequate planning of the construction site layout. [5] indicated that site layout planning is a complex problem, due to the existence of several large tasks that need to be performed. [6] demonstrated that utilizing site space efficiently to locate resources and facilities over the duration of a project is a complicated dilemma.

2.1. Optimization models based on travel cost distance only

In general, most of the existing site layout planning studies consider the travel cost distance as the most significant objective function. They also apply several algorithms to optimize and accommodate construction facilities. [7] indicated that site layout models can be categorized into two classes. One is the static model, i.e. changes over time are not considered. The other is the dynamic model, i.e. changes over time are considered. [34,35] classified the algorithms used to solve facility layout problem into four categories: construction algorithms, improvement algorithms, hybrid algorithms and graph theoretic algorithms. [34] made comparison among twelve algorithms to examine their efficiency based on computation time and the accuracy of the solution. [8] noted that the meta-heuristic methods such as genetic algorithms (GAs), simulation techniques and ant colony optimization are most common algorithms used for site layout planning. [33] developed a hybrid model that integrates genetic algorithm with max-min ant system. The results of this hybrid model provide better optimal solution than utilizing traditional genetic algorithm.

[9] developed an evolution model called EvoSite. It implements a GA when searching for the optimum layout. [10] investigated the capabilities of a GA in finding the optimal solution for site layout problems. They found that when the ratio between the area of total facilities and the site area did not exceed 60%, the algorithm produces a solution that is considered very close to the optimal solution. [1] presented a model based on approximate dynamic programming (ADP) in order to optimize dynamic site layout of construction projects. [11] made a comparison between a GA model and ADP by considering two criteria: the effectiveness of optimal solution attainment and the efficiency of minimizing the computation time. They found that ADP was more efficient than the GA. However, GAs will continue to be a valuable optimization method due to their simplicity. [6] illustrated a procedure based on linear programming for dynamic site layout, by minimizing the travel distance and relocation costs among all facilities. [12] developed an innovative dynamic model to seek the optimal positions of the facilities. The model is derived from the principles of an energy dominating physical system. The strength of this model is its ability to assign space to facilities when they are required on the site and allows for the reuse of the space over time.

Furthermore, several researchers have used advanced technologies such as the geographic information system (GIS) and building information modeling (BIM) for site management. [13,14] developed a site layout system called ArcSite. The proposed model uses the elimination searching technique to generate the optimal position for each facility. [15] presented a framework for the continuous tracking of the 4D status of a dynamic construction site, utilizing radio frequency identification (RFID), the global positioning system (GPS) and the GIS, in order to achieve project objectives. [16] utilized GIS for determining the optimal layout of a haul route for large earthmoving projects. [17] described the problems associated with site layout planning and developed a model utilizing building information modeling (BIM) to generate a 3D site layout plan.

2.2. Optimization models for consideration of safety issues

[18] proposed model for site layout planning that considers other relevant criteria, rather than distance, such as site safety and productivity. The GA was used to achieve an optimal site layout. [5] developed an optimization site layout model by utilizing a GA and considering the actual route between facilities and safety aspects. [4] presented a model capable of maximizing construction safety and minimizing travel costs within a construction site. The model considers only crane safety operation and hazardous materials as safety criteria. Although the model did not take into account hazards from all other construction facilities, but it is still vital because it illustrated the trade-off between safety and travel costs. [19] proposed a planning method in order to protect workers from injuries and keep them at a safe distance from each other. The proposed method depends on the assumption that the hazardous situation is a result of the interaction between the reinforcing and counteracting characteristics of the workers. Moreover, 3D time-space diagram is embraced in the methodology to analyze the dynamic movement of workers on the construction site. [20,21] indicated that if the initial accident or hazard occurs at industrial plants, and then starts to

propagate to other objects and facilities within the plants, it will cause damages to the targets erected in the vicinity of the hazard sources. It may also cause a new sequence of damages and cascading effect called "domino effect".

However, up to now, only a few studies have been devoted to the generation of efficient models for site layout planning, capable of avoiding, or at least diminishing, risk of natural or technological hazard and subsequent disasters. Moreover, most of the previous studies did not identify the effect of space configurations on the severity of the risks within the site. The proposed model in this research overcomes the deficiencies of the existing optimization models, as the layout optimization now depends on the hazard and the vulnerability of the facilities, instead of transportation cost. Moreover, the risk is visualized within a construction site by considering the space configuration and visibility as a penalty factor in estimating the risk at each position within a site.

Therefore, the main goals of our research concern:

- The application of a space syntax concept that deals with space configuration, proving that it is an efficient method for understanding, accommodating and modeling spatial analysis problems [24].
- The implementing of an interaction matrix technique to determine the potential global impact for each construction facility in the project.
- The use of a differential evolution optimization technique to optimize site layout facilities based on interaction matrices.
- The use of GIS capabilities to analyze spatial datasets and generate a risk map for the construction site.

3. Methodology

The specified model consists of four phases, as shown in Fig. 1: (1) creating interaction matrices for the hazards and vulnerabilities among facilities; (2) identifying decision variables, constraints and the objective function for optimization utilizing the differential evolution technique; (3) implementing space syntax principles to determine the influence of space configuration and (4) importing the data from previous steps to the GIS to generate a construction site risk map.

The proposed model aims to find the best position for each facility, within a construction site, in order to minimize the risk. It is based on the hazards generated by the potential sources, the vulnerability of the potential targets and the hazard attenuation value.

The decision variables are represented by the (x, y) coordinates of each facility. The evolutionary algorithm is utilized to determine these coordinates considering both the boundary and overlapping constraints. Once the coordinates are identified, the optimal risk matrix and optimal site layout can be generated. The optimal risk matrix is utilized to find the potential global impact for each facility. Afterwards, the space syntax analysis is conducted on the optimal site layout to determine the mean depth for each position within a construction site. Finally, the optimal site layout, potential global impact for each facility and visual mean depth are integrated together, utilizing the GIS to create a spatial risk map, as illustrated in the following sections.

3.1. Interaction matrices

The framework for generating the hazard and vulnerability interaction matrices consists of several steps. It aims to evaluate the hazard generated by each facility compared to the other facilities. It can be adapted to consider different natural hazards that may happen on a construction site, i.e. fire, explosions, thermal flux and blast waves, for instance. Moreover, it is possible to identify the vulnerability of targets within a site with respect to the hazards generated from each source. The vulnerability of each target depends on its capacity to resist various hazard values generated by surrounding sources. In the framework, the global risk for each facility can be identified by the convolution product between hazards generated by the sources and the vulnerability of the targets.

3.1.1. Modeling hazard interaction matrix

Suppose hazard interaction matrix between construction facilities **H**, and n is the total number of construction facilities that must be accommodated within a construction site. Hence, an (n x n) matrix must be developed. Several steps should be followed in order to model hazard interaction matrix [20,21,23]:

1. Identify the construction components that will be erected within the construction site.
2. Identify the kind of hazards that may happen in a construction site. It is assumed that, there is a same kind of hazard effect generated from all sources.
3. Evaluate the hazard generated by each facility (i) using arbitrary relative scale measurement categories specified in Table 1, where 0 represents the lowest hazard level, while 4 represents the highest hazard level. In addition, the diagonal of the matrix is filled with these values as shown in Eq. (1), where h_{11} represents the hazard generated from source 1, h_{ii} represents the hazard generated from source (i) and so on. In fact, while this value seems such as the source (i) interacting with itself, this just indicates that the intensity of the hazard is the highest at the source itself and declines as it becomes far away from the hazard source.

$$\mathbf{H} = \begin{bmatrix} \boldsymbol{h}_{11} & \dots & \\ \vdots & \boldsymbol{h}_{ii} & \vdots \\ & \dots & \boldsymbol{h}_{nn} \end{bmatrix} \tag{1}$$

4. To find the remaining values of the hazard interaction matrix, for the sake of simplicity, it is assumed that there is a linear attenuation law between hazard decay and distance, i.e. a linear relationship between the hazard interaction values ($\mathbf{h_{ij}}$) and the distance ($\mathbf{d_{ij}}$) to the target, therefore, the hazard from source (i) on target (j) decreases as target (j) is located far away from source (i). Thus, the hazard decay, which is represented by the slope of linearity decreasing (tan α) should be identified, as shown in Fig. 2, based on the nature of hazards, whether is it thermal flux, heat pressure or any other natural hazards effect. Furthermore, specific studies of the attenuation can be adopted depending on the nature of the hazard [20,21,22,23]. Eqs. (2)–(5) explain the linear attenuation of hazard, whereas Eq. (6) displays the completed hazard interaction matrix. In addition, Eqs. (7)–(9) are utilized to normalize the hazard interaction matrix.

$$h_{ij} = \max\begin{cases} \mathrm{h}_i^0 + \dfrac{\Delta \mathrm{H}}{\Delta \mathrm{d}} * \mathrm{d_{ij}} * \beta \\ 0 \end{cases} \tag{2}$$

$$h_i^0 = h_i|_{d=0} = h_{ii} \tag{3}$$

$$\mathrm{d_{ij}} = \sqrt{(\mathrm{x_i}-\mathrm{x_j})^2 + \left(\mathrm{y_i}-\mathrm{y_j}\right)^2} \tag{4}$$

$$\beta_{\mathrm{ij}} = \begin{cases} 1, & \text{if } \mathrm{i} \neq \mathrm{j} \\ 0, & \text{otherwise} \end{cases} \tag{5}$$

$$\mathbf{H} = \begin{bmatrix} h_{11} & \dots & h_{1n} \\ \vdots & h_{ij} & \vdots \\ h_{n1} & \dots & h_{nn} \end{bmatrix} \tag{6}$$

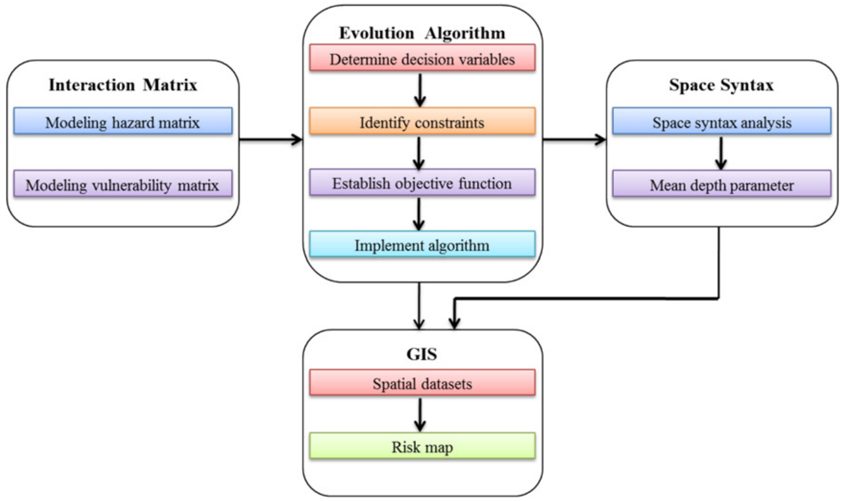

Fig. 1. Methodology flowchart.

$$\mathbf{H}^* = \begin{bmatrix} h^*_{11} & \cdots & h^*_{1n} \\ \vdots & h^*_{ij} & \vdots \\ h^*_{n1} & \cdots & h^*_{nn} \end{bmatrix} \tag{7}$$

$$h^*_{ij} = \frac{h_{ij}}{\max\left[h^0_i\right]} \tag{8}$$

$$\mathbf{H} = \max\left[h^0_i\right] \cdot \boldsymbol{H}^* = \max\left[h^0_i\right] \cdot \begin{bmatrix} \mathrm{h}^*_{11} & \cdots & \mathrm{h}^*_{1n} \\ \vdots & \mathrm{h}^*_{ij} & \vdots \\ \mathrm{h}^*_{n1} & \cdots & \mathrm{h}^*_{nn} \end{bmatrix} \tag{9}$$

Where:

- $\mathbf{H}$ is the hazard interaction matrix
- h_{ii} is the potential hazard of source (i) on the target (i), i.e. the effect of source on itself.
- $h_i|_{d=0} = h^0_i$ is the potential hazard generated from facility (i) at distance (d = 0)
- h_{ij} is the hazard interaction value between facilities (i) and (j), i.e. the effect of source (i) on the target (j)
- $\frac{\Delta H}{\Delta d}$ is the amount of hazard attenuation with distance (hazard decay).
- β is a factor utilized to consider the case when the hazard evaluation value is maximum at d = 0 (i.e. to consider the case when i = j).
- $\mathrm{d_{ij}}$ is the Euclidean distance between facilities (i) and (j).
- $\mathrm{x_i}, y_i, x_j, y_j$ is the coordinates of facilities (i) and (j).
- n is the total number of facilities in the construction site
- $\mathbf{H}^*$ is the normalized hazard interaction matrix
- h^*_{ij} is the normalized hazard interaction value between facilities (i) and (j), $\forall\, \mathrm{h}^*_{ij} \in [0,1]$
- $\max[h^0_i]$ is the maximum value of potential hazard generated from facility (i) at distance 0 among all facilities, i.e. the maximum value among all diagonal values in the hazard interaction matrix.

Table 1
Hazard interaction scale measurements.

Hazard level	Details
0	No hazard
1	Low hazard
2	Moderate hazard
3	High hazard
4	Very high hazard

3.1.2. Modeling vulnerability interaction matrix

In order to develop the vulnerability modeling of whole targets within a site to the hazards generated from each source, suppose vulnerability interaction matrix between construction facilities **V**. The vulnerability of each target depends on its ability to resist various hazard values generated by surrounding sources. However, as the hazards are physical phenomena and are not explicitly chosen due to general validity requirements, it is assumed, in this paper, that the conditional vulnerability is a linear function of hazard value, as shown in Fig. 3. According to [21] the main shortcomings of the previous studies in evaluating construction vulnerability attributed to: inability of these studies in providing practical and effective value of structural vulnerability; furthermore, the vulnerability does not evolve with the hazard level. Therefore, [21] expressed the vulnerability as damage functions, which are considered as function of hazard intensity. More sophisticated variations of the conditional vulnerability, according to the hazard intensity, can be collected from investigations on specific systems such as, masonry under floods or quakes, or industrial metal tanks under tsunamis [20,21,22,23]. Eqs. (10)–(12) illustrate the conditional vulnerability.

$$\mathbf{V} = \begin{bmatrix} \mathrm{v}_{11} & \cdots & \mathrm{v}_{1n} \\ \vdots & \mathrm{v}_{ji} & \vdots \\ \mathrm{v}_{n1} & \cdots & \mathrm{v}_{nn} \end{bmatrix} \tag{10}$$

Since the vulnerability is assumed as function of hazard as shown in Fig. 3, then:

$$\mathrm{v}_{ji} = h_{ij} \tag{11}$$

$$\mathbf{V} = \mathbf{H}^T \tag{12}$$

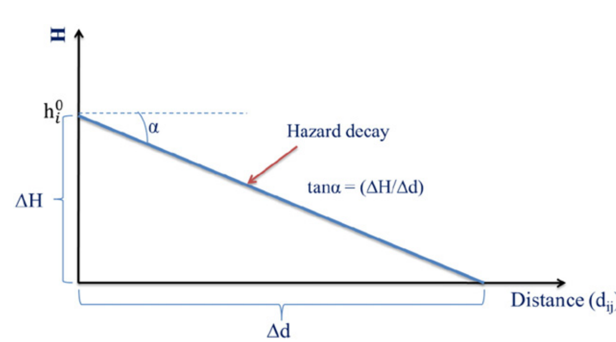

Fig. 2. Hazard decay as a linear function of distance.

Where:

$\mathbf{V}$	is the vulnerability interaction matrix
$\mathbf{H}^T$	is the hazard transpose interaction matrix
v_{ji}	is the vulnerability of target (j) to the hazard generated by source (i).

3.2. Optimization technique (evolutionary algorithm)

Evolutionary algorithms are useful methods for solving complex optimization problems that are not suitable for gradient based algorithms. The idea behind evolutionary algorithms is derived from Darwin's principle which relies on the survival of the fittest. These algorithms imitate the optimization process in nature. The biological species are optimized in order to maximize the survival of the fittest, which leads to an enhancement in the quality of that generation. As the evolutionary algorithm (Genetic Algorithm) is a very common technique for solving optimization problems [5,9,10,25,26], it is adopted in the present research.

3.2.1. Evolutionary approach

The first step to implement the evolutionary optimization technique is to design particular chromosomes containing genes of the problem decision variables as shown in Fig. 4. It is obvious from this figure that each successive genes pair represents the x and y coordinates for facility (i). Moreover, the number of decision variables are equal to the number of facilities (n) multiplied by two (the number of variables = 2n). In the current model the decision variables (genes) are set as numerical values (real numbers).

Generally, GAs work with a collection of chromosomes called population. The chromosomes are evaluated through process called fitness function to examine the convenient of the solution. The genetic operators called "crossover and mutation" are applied. In crossover, some chromosomes in population are mate to generate new chromosomes called offspring. Offspring inherit merits from their parents. In mutation, few chromosomes are mutate in their genes. The chromosomes undergo to crossover and mutation operations are randomly selected and controlled through crossover rate and mutation rate. The probability of chromosome in the current population, to be appearing again in the next generation is directly proportional with the fitness value. After several generations, the optimal solution will be obtained. In the current model, the differential evolution algorithm is adopted to perform optimization process. It is available at Science Python (SciPy) library. According to [36,37,38], for each generation, the mutation operation is conducted for each candidate solution through mixing it with other candidate solutions to create trial chromosome as shown in Fig. 4. In mutation operation, two chromosomes are randomly selected from the population, and then the difference between them is determined (i.e. difference chromosome is created). The resulted difference chromosome is scaled based on user defined parameter called mutation parameter. Afterwards, the scaled difference chromosome is added to the best chromosome in the population to generate new chromosome called mutant chromosome. This later is subjected to discrete recombination with the parent chromosome to create trial chromosome using crossover parameter. This trial chromosome is undergoing to fitness evaluation. If it is better than the parent, it will occupy its position. In addition, if the trial chromosome is better than the best chromosome in the generation, it will take its place too.

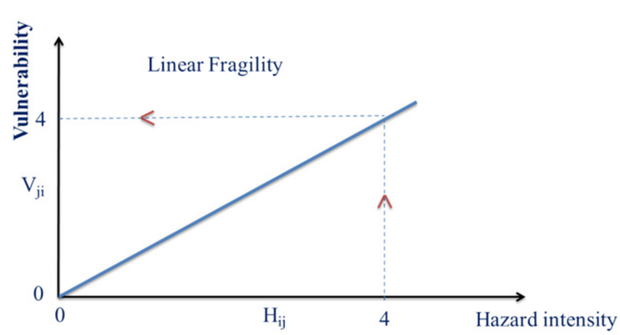

Fig. 3. Vulnerability as a linear function of hazard value.

3.2.2. Optimization model development

3.2.2.1. Site and facility representation. In the proposed model, the construction site is represented as a rectangle with length (L) and width (W). The coordinate system (x, y) is created. The boundaries of the construction site along the x axis are x_1 and x_2, while the boundaries along the y axis are y_1 and y_2, as displayed in Fig. 5. Also, let the number of construction facilities to be located in construction sites be (n). The construction facilities have different sizes and are represented as rectangles too, with length ($\updownarrow_i$) and width (w_i), where i = 1, 2, …, n. The coordinates of the centroid of the facility (i) is (x_i, y_i). These coordinates are the decision variables of the problem [27]. Fig. 5 displays the model components representation that involves: site boundaries and its dimensions, construction facilities and their dimensions, and the decision variables (x_i, y_i) for facility (i).

3.2.2.2. Objective function. It is important to develop a model able to minimize risks within a construction site, and identify the best layout plan that shows the spatial disparity of the global impact of each facility within the whole site.

The objective function aims minimizing the risk due to potential hazards. Therefore, it is required to minimize the global potential impact of each facility within the construction site. This is reached by identifying the best position for each facility, where the total risk in the site is at the minimum value. The distance between two facilities has been expressed as Euclidean distance (the shortest straight line distance between facilities). As presented previously, the conditional vulnerability is considered as a damage function and expressed as a function of hazard intensity. The workflow of objective function derivation is shown in Eqs. (13)–(16):

$$\boldsymbol{\mathcal{R}isk} = \mathbf{H} * \mathbf{V} \tag{13}$$

Since, $\mathbf{V} = \boldsymbol{H}^T$ as shown in Eq. (12), therefore:

$$\boldsymbol{\mathcal{R}isk} = \mathbf{H} * \boldsymbol{H}^{\boldsymbol{T}} \tag{14}$$

For sake of simplicity, it is assumed that the objects hazards are not happening simultaneously. Therefore, the total risk from all objects is a cumulative risk generated from each object as shown in Eq. (15). Moreover, Eq. (16) displays the objective function of site layout optimization problem.

$$Total\ \mathcal{R}isk = \sum_{i=1}^{n}\sum_{j=1}^{n}(\mathcal{R}_{ij}) \tag{15}$$

$$\mathcal{M}inimize \sum_{i=1}^{n}\sum_{j=1}^{n}(\mathcal{R}_{ij}) \tag{16}$$

Where:

$\boldsymbol{\mathcal{R}isk}$	is the risk interaction matrix among facilities.
$\mathcal{R}_{ij}$	is the risk interaction value due to the hazard generated from source (i) and vulnerability of the target (j).

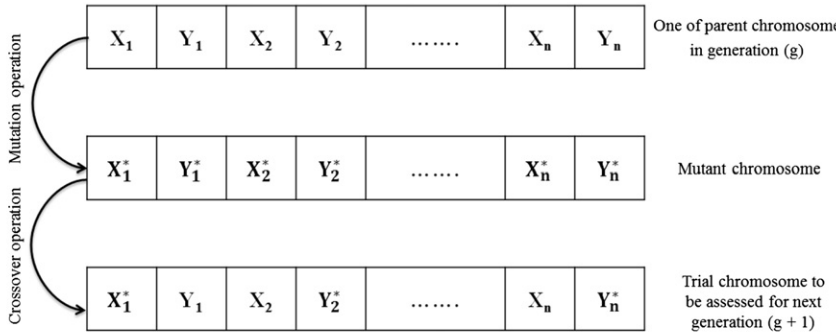

Fig. 4. Illustration of the decision variable chromosomes.

3.2.2.3. Model layout constraints. Usually, it is not possible to accommodate facilities in any arbitrary location. In fact, there are some constraints that should be considered to avoid infeasible solutions. The constraints that are considered herein are construction site boundary and overlapping constraints:

- A boundary constraint is used to guarantee that all facilities are located within the construction site, as shown in Fig. 6. For instance, facility (1) satisfies the boundary constraint, whereas facilities (2) and (3) violate that constraint. However, the facilities are not considered violating the boundary constraints if conditions in Eqs. (17)–(20) are satisfied [27].

$$x_1 + \frac{\ell_i}{2} - x_i \leq 0.0 \tag{17}$$

$$x_i + \frac{\ell_i}{2} - x_2 \leq 0.0 \tag{18}$$

$$y_1 + \frac{w_i}{2} - y_i \leq 0.0 \tag{19}$$

$$y_i + \frac{w_i}{2} - y_2 \leq 0.0 \tag{20}$$

- An overlap constraint is enforced to guarantee that there is no overlapping between any pair of facilities. As shown in Fig. 7, facility (1) satisfies the constraint, whereas facilities (2) and (3) violate the constraint. No overlapping is achieved, if at least one of the conditions in both Eqs. (21) and (22) are satisfied [27].

$$-|x_i - x_j| + \frac{\ell_i}{2} + \frac{\ell_j}{2} \leq 0.0 \tag{21}$$

$$-|y_i - y_j| + \frac{w_i}{2} + \frac{w_j}{2} \leq 0.0 \tag{22}$$

Where:

x_i, x_j, y_i and y_j are the coordinates for facilities (i) and (j).
ℓ_i, ℓ_j, w_i, w_j are the lengths and widths of facilities (i) and (j).

Through implementing the optimization evolutionary technique, each facility will start being located at a position inside the construction site. Once the optimization achieves the described utility function and constraints, the optimal risk matrix will be generated. From this matrix, the overall potential global impact of each facility can be determined through utilizing Eqs. (23)–(27).

$$\boldsymbol{\mathcal{R}isk}_{opt} = \begin{bmatrix} \mathcal{R}_{11} & \dots & \mathcal{R}_{1n} \\ \vdots & \mathcal{R}_{ij} & \vdots \\ \mathcal{R}_{n1} & \dots & \mathcal{R}_{nn} \end{bmatrix} \tag{23}$$

$$\overline{\mathcal{R}}_j = \sum_{i=1}^{n} \mathcal{R}_{ij} \quad , \forall j \in \{1, 2, \dots, n\} \tag{24}$$

$$\overline{\mathcal{R}}_i = \sum_{j=1}^{n} \mathcal{R}_{ij} \quad , \forall i \in \{1, 2, \dots, n\} \tag{25}$$

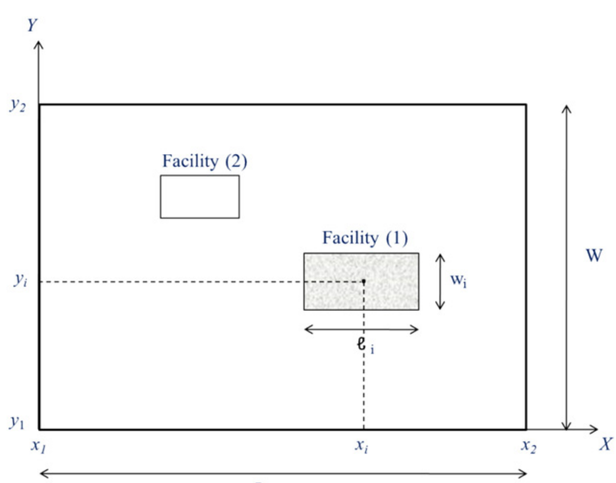

Fig. 5. Representation of the construction site and facilities.

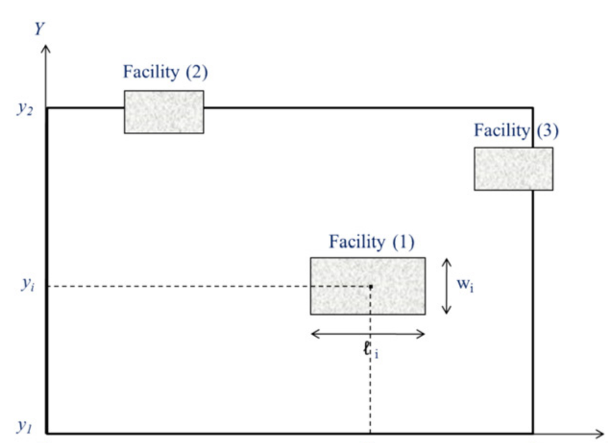

Fig. 6. Illustration of the boundary constraint.

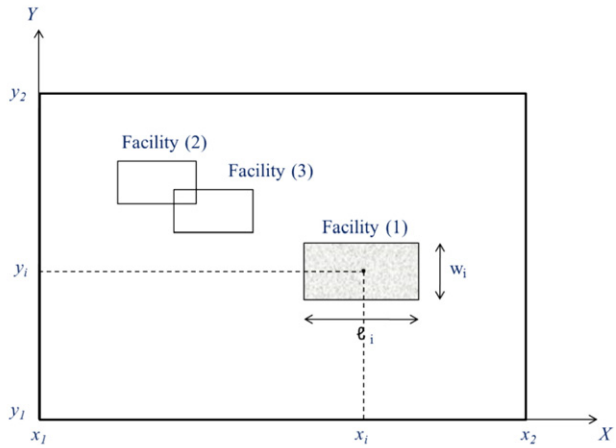

Fig. 7. Illustration of the overlapping constraint.

$$\varkappa_i^* = \overline{\mathcal{R}}_j + \overline{\mathcal{R}}_i \quad , \forall i, j \in \{1, 2, \dots, n\} \tag{26}$$

$$\psi_i = \frac{\varkappa_i^*}{\sum_{i=1}^{n} \varkappa_i^*} \quad , \forall i \in \{1, 2, \dots, n\} \tag{27}$$

Where:

$\mathcal{R}isk_{opt}$	is the optimal interaction risk matrix
$\overline{\mathcal{R}}_i$	is the potential risk resulted from the hazard of each source (i) in the site.
$\overline{\mathcal{R}}_j$	is potential sensitivity of each target (j) to the hazards sources.
$\varkappa_i^*$	is the potential global impact of each object (i) on the whole site.
ψ_i	is the relative potential global impact of each object (i) on the whole site

3.3. Space syntax

Space syntax is a spatial analysis technique that was developed to understand and realize the spatial patterns and space configurations of modern cities based on connectivity graph representation [28]. The spatial analysis in this research relies on the delineation of least risk paths. These paths will have high visibility and connectivity in order to facilitate site evacuation in case of hazard occurrence. Referring to [24], the notion in space syntax model depends on two fundamental steps:

- Dividing large scale space (free space) into a limited number of small spaces. The awareness of small scale spaces affords prequalification to the awareness of large scale one.
- Connecting of the small spaces together to create a connectivity graph. It constitutes the basis to compute a set of spatial property parameters. Mean depth is one of the most significant parameters that must be considered to establish the spatial variability of risk.

Depth can be defined as the number of steps from a considered node to all other nodes. A node can be considered either deep or shallow based on the number of steps separating it from all other nodes. As the evacuation process will be considered in evaluating and visualizing the risk within a construction site, the deep positions will have higher risk compared to shallow ones due to the limited connectivity and visibility with other locations, which in turn will hinder the evacuation process. Furthermore, the actual risk is amplified by utilizing mean depth as a penalty factor. Mean depth is high for deeper positions and low for integrated or shallow positions, as explained in detail in the next section. The depth and mean depth of a node can be computed using Eqs. (28) and (29) respectively, obtained from [24].

$$\delta_k = \sum_{j=1}^{N} S_{kj} \tag{28}$$

$$\overline{\delta}_k = \frac{\sum_{j=1}^{N} S_{kj}}{N-1} \tag{29}$$

Where:

δ_k	is the depth of node (k).
S_{kj}	is the shortest distance (steps) between two nodes (k and j) in a connectivity graph, then the total depth of node (k) is the sum of the steps.
$\overline{\delta}_k$	is the mean depth of node (k).
N	is the total number of nodes.

Depth map analysis software was used to determine mean depth values that will be used to generate the spatial variability map of risk within a construction site.

3.4. GIS datasets

For sake of simplicity, we assume that the spaces in the site are subjected to the same vulnerability and they are affected by their surrounding objects. The construction site and facilities have been converted to raster. Cells representing facilities have values equal to relative potential global impact of that facility (z_i). These cells are used to determine the potential global risk for each unknown node ($\mathcal{Z}_k$) in the site and generate the spatial risk map. To do so, one common interpolation techniques called inverse distance weighting (IDW) was utilized. The interpolation technique is based on the concept that spatially distributed elements

Table 2
Facility dimensions and description.

Facility	Length "ℓ" (m)	Width "w" (m)	Description	Location attribute: fixed or movable
F_1	2	1	Electric generator	Movable
F_2	7	3	Labor services	Movable
F_3	10	6	Concrete plant	Movable
F_4	12	5	Job office 1	Movable
F_5	5	12	Job office 2	Movable
F_6	8	20	Steel storage	Movable
F_7	2	1	Fuel storage	Movable
F_8	8	8	Tower crane	Fixed (32,30)[a]
F_9	26	50	Building under construction	Fixed (14,28)[a]

[a] The coordinates of predefined (fixed) objects.

are spatially correlated. The IDW technique assumes that the weight of each interpolated sample point vanishes with distance. Therefore, if the sample point is too close to the unknown cell, then it will has higher weight in determining ($\mathcal{Z}_k$), as shown in Eq. (30). Moreover, Eq. (31) is utilized to estimate the potential global risk ($\mathcal{Z}_k$) for unknown cells.

$$w_i = \frac{1}{d_{ik}^{p}} \tag{30}$$

$$\mathcal{Z}_k = \frac{\sum_{i=1}^{m} z_i w_i}{\sum_{i=1}^{m} w_i} \tag{31}$$

Where:

$\mathcal{Z}_k$	is the potential global risk for cell (k) in the site
z_i	is a relative potential global impact value for cell (i) used as sample interpolated point.
w_i	is the weight of sample point (i)
d_{ik}	is the distance between the sample interpolated point (i) and the unknown node (k)
p	is the power value parameter ($p \geq 1$).
m	is the number of sample interpolated points used to estimate unknown node (k).

The mean depth ($\bar{\delta}_k$) results are imported to the GIS in order to perform spatial analysis and generate the visual map for risk within a construction site. As the evacuation process will be considered in evaluating and visualizing the risk within a construction site, the actual risk is amplified by utilizing a penalty factor that has a high value for deeper locations and a low value for integrated or shallow locations. Therefore, it is assumed that the risk amplification factor ($\mathcal{R}_{af_k}$) can be expressed using Eq. (32):

$$\mathcal{R}_{af_k} = \mathcal{Z}_k * \bar{\delta}_k \tag{32}$$

The spatial analyst tools in ArcGIS were utilized to find amplified risk for each node (k) within a construction site. As noted in Eq. (32), the actual risk for any point within a construction site depends on two values, the potential global risk of the node and the mean depth of the node. Therefore, when the node becomes too close to the facilities with highest global potential impact, the potential global risk at that node will be high compared to those located far away from these facilities. Moreover, as the node is too segregated (i.e. has a high mean depth value), it will have a higher risk, since the visibility from this node is very limited, which in turn will impact the identification of the developed actual route for evacuation in the case of emergency compared to those having good visibility and low mean depth value. In addition, the risk can also be expressed as the probability of occurrence of a limit state function. In that case, the risk (Eq. (32)) should be normalized and take values within [0–1]. Otherwise, Eq. (32) can be considered as a risk index that could be used for comparative purposes, i.e. to compare various solutions and find the optimal one.

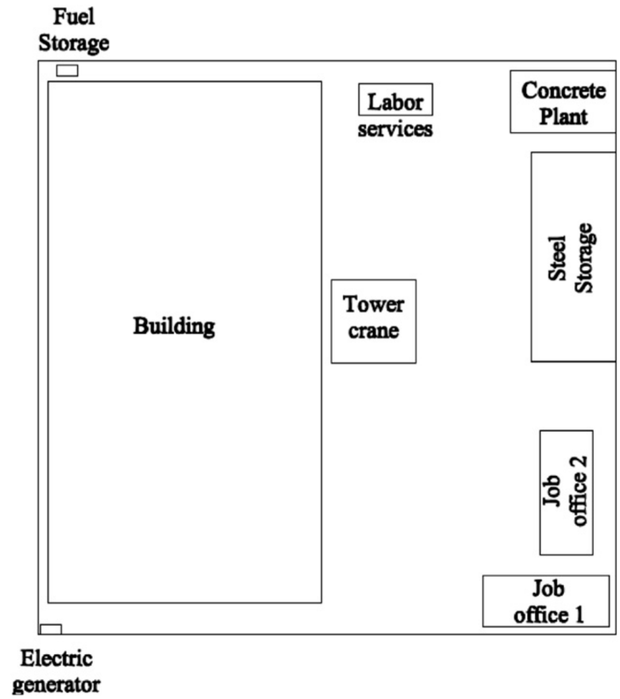

Fig. 8. Layout of the optimal facility positions.

4. Model implementation

A case study is implemented in order to validate the proposed model by minimizing and visualizing the risk of a construction site. The dimensions of the site are 55 × 55 m. The dimensions and nature of the required facilities are shown in Table 2. It contains nine facilities, such that facilities (F_1), (F_7) and (F_8) represent the highest sources of hazard and threat within the construction site. Furthermore, the objects within the construction site are categorized into fixed or movable. Actually, the locations of building under construction, and sometimes the tower crane, are fixed prior to the construction launch and these locations cannot be changed. They are considered as fixed objects. Other facilities like, for example, job offices and storage areas can be erected at their optimal position within the construction site, i.e. to minimize a total risk, they are considered as movable. The Python language platform was utilized to execute the optimization process. A personal computer with 2.4 GHz Intel(R) core(TM) i7-5500U CPU, and 16 GB of Ram was utilized. It took 150 s (data input, CPU time, mapping and results output) to find the optimal layout of nine facilities.

The proposed model requests that the manager identifies several inputs: (1) the nature of the hazards, which is considered, in this example, as thermal flux; (2) the potential hazards and threats from each facility in order to fill the diagonal values in the hazard interaction matrix, as

Table 3
Maximum hazard intensity from each facility.

Facility	F_1	F_2	F_3	F_4	F_5	F_6	F_7	F_8	F_9
F_1	4								
F_2		1							
F_3			3						
F_4				2					
F_5					2				
F_6						2			
F_7							4		
F_8								4	
F_9									2

Table 4
Coordinates of each object center.

Facility	Coordinates (x, y) [Units: m]
F_1	(1.25,0.5)
F_2	(34.1,51.3)
F_3	(50,51.1)
F_4	(48.4,3.2)
F_5	(50.3,13.6)
F_6	(51,36.2)
F_7	(2.8,54.1)
F_8	(32,30)
F_9	(14,28)

Table 5
Normalized potential global impact of the facilities.

Facility	Overall weight	Normalized weight
F_1	0.159	0.883
F_2	0.061	0.339
F_3	0.116	0.644
F_4	0.077	0.427
F_5	0.080	0.444
F_6	0.081	0.450
F_7	0.163	0.906
F_8	0.180	1.000
F_9	0.083	0.461

Table 7
Non-normalized optimal interaction risk matrix.

Facility	F_1	F_2	F_3	F_4	F_5	F_6	F_7	F_8	F_9
F_1	16.00	11.53	10.88	12.44	12.20	11.48	12.00	12.77	13.66
F_2	0.16	1.00	0.71	0.25	0.35	0.60	0.47	0.62	0.48
F_3	5.28	8.07	9.00	6.36	6.89	8.13	6.39	7.41	6.62
F_4	2.33	2.25	2.31	4.00	3.59	2.79	1.73	2.84	2.48
F_5	2.23	2.53	2.64	3.59	4.00	3.15	1.89	3.08	2.59
F_6	1.93	3.15	3.43	2.79	3.15	4.00	2.21	3.24	2.63
F_7	12.00	13.59	12.44	11.00	11.40	12.16	16.00	13.12	13.82
F_8	12.77	14.33	13.86	13.59	14.10	14.45	13.12	16.00	14.59
F_9	2.87	2.87	2.48	2.48	2.59	2.63	2.95	3.31	4.00

shown in Table 3; (3) the hazard attenuation (hazard decay) which is identified as 0.01. This can be changed based on the kind of hazard and to perform a sensitivity analysis of the hazard [20−23]. In this example, all input data are used to optimize the location of facilities within a site and to generate an actual risk map. This map visualizes how risk varies from one position to another and identifies the most risky locations within a site. For optimization purposes, the differential evolution technique was used. The initial population consists of 100 chromosomes.

The mutation and crossover operators are implemented to create the next generations with better fitness, until finding the optimal solution. Several runs were performed in order to get the optimal location of facilities and determine the potential global impact that each facility has within a construction site. The relative disposal between the facilities is found as the optimization solution. The absolute location therefore will be defined once any one of the facilities is chosen. For instance, one possible absolute location and the results for this solution are displayed in Fig. 8. It shows the optimal disposal location of facilities. In addition, Tables 4–7 present the optimized coordinates of the object, normalized potential global impact for each facility, the distance between facilities and the optimal interaction risk matrix, respectively.

For the case study, it appears that facility (F_8) has the highest potential global impact within the site with a value equal to 18.0%, followed by facilities (F_7) and (F_1), respectively. Furthermore, it is noticeable that facilities (F_4), (F_5), (F_6) and (F_9) have approximately the same potential global impact value (about 8.0%). Also, the potential global impact of facility (F_2) is the lowest among all other facilities with a value of 6.1%. Hence, it can be noticed that the electric generator (F_1) and fuel storage (F_7) are located far away from the other facilities. The position of the tower crane (F_8) cannot be changed, since it is a fixed facility, as shown in Fig. 8. This indicates that the risk consequences from facilities (F_1), (F_7) and (F_8) are the highest. In addition, the risk generated from other facilities are either moderate such as facilities (F_4), (F_5), (F_6) and (F_9) or low like facility (F_2) or between moderate and high like facility (F_3). This can be concluded from Fig. 9 which displays the spatial variability of the potential global risk. This later is estimated, utilizing IDW, based on the potential global impact of the facilities. Fig. 9 confirms that the nodes closer to the facilities with the highest potential global impact will have a higher value of potential risk compared to those located far away. It is therefore obvious

Table 6
Distances [m] between facilities.

Facility	F_1	F_2	F_3	F_4	F_5	F_6	F_7	F_8	F_9
F_1	0	60.49	70.22	47.26	50.76	61.13	53.60	42.61	30.47
F_2		0	15.88	50.16	41.00	22.58	31.38	21.40	30.64
F_3			0	47.85	37.44	14.90	47.23	27.70	42.65
F_4				0	10.56	33.05	68.31	31.41	42.52
F_5					0	22.57	62.36	24.55	39.10
F_6						0	51.26	19.87	37.34
F_7							0	37.82	28.23
F_8								0	18.09
F_9									0

from the map that the areas adjacent to facilities (F_8) at the middle of the site, (F_7) at the top left of the site and (F_1) at the bottom left of the site are the most risky positions. It also appears that the areas adjacent to facility (F_2) have the lowest risk. Finally all other areas are of intermediate risk due to the proximity to facilities with moderate potential global impact.

The mean depth results are displayed in Fig. 10. It can be noticed that the positions with higher integration and low mean depth values have lower risk. These locations are not segregated and have good visibility to other areas. However, the positions that have low integration and high mean depth values are of higher risk due to the limited visibility to other locations. These locations can be considered as segregated one. The map shown in Fig. 10 indicates that the following positions are segregated and have higher risk, compared to others due to limited visibility and connectivity with other locations:

- Along the left side of the site behind the building under construction (F_9).
- Bottom left of the site beside electric generator (F_1).
- Top left of the site, adjacent to fuel storage facility (F_7).
- Bottom right near job offices (F_4) and (F_5).

Moreover, the mean depth values at the middle of the construction site (Fig. 10) are low due to good visibility and high connectivity. Therefore, evacuation from these areas will be easier than evacuation from other locations, in case of emergency.

The final map, combining the site potential global risk ($\mathcal{Z}_k$) and site mean depth penalty factor ($\overline{\delta}_k$), is shown in Fig. 11. This displays the spatial variability of actual risk within a construction site. The zones that have high values indicate higher risk and are displayed in red and

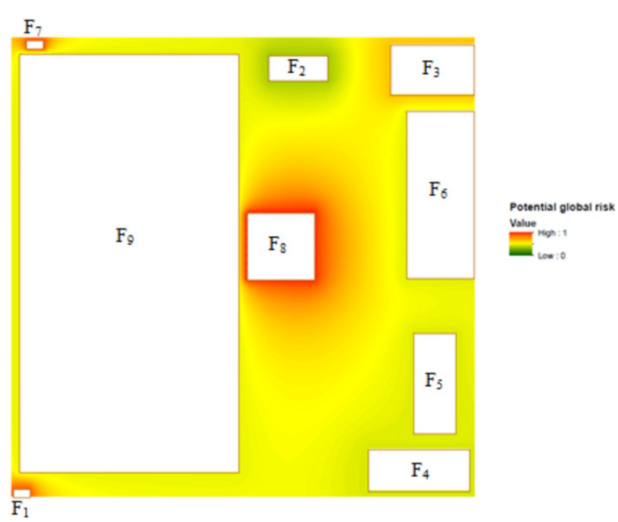

Fig. 9. Map of site spatial variability of the potential global risk ($\mathcal{Z}_k$).

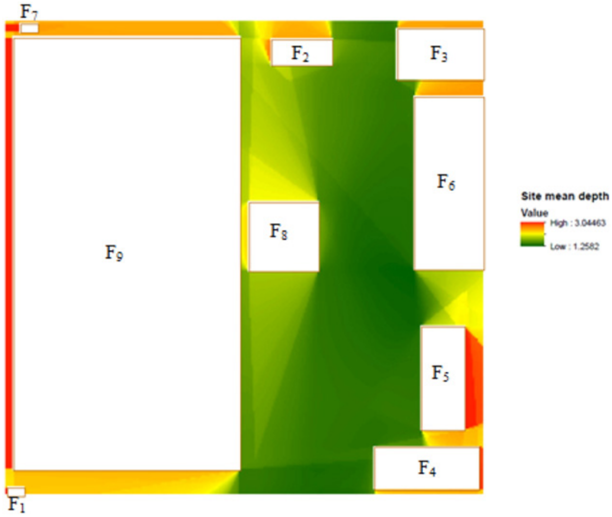

Fig. 10. Map of site mean depth ($\bar{\delta}_k$).

appear at the top left of the site: adjacent to facility (F_7), bottom left of the site, near facility (F_1) and finally around facility (F_8) in the middle of the construction site. This is due to the high potential global impact of these facilities. Moreover, Fig. 11 reveals that the risk behind the building under construction (F_9) along the left side of the site, bottom right adjacent to the job offices and areas adjacent to the concrete plant facility (F_3) are moderate. This is due to low visibility and connectivity. Finally, the map shows that the remaining zones within the site have lower risk values. These zones are displayed in green and appear almost within the middle of the site. This is due to the fact that their positions are far away from facilities with highest potential global impact. Also, these zones have good visibility, high integration, high connectivity and low mean depth values compared to the most risky ones.

5. Conclusions

This paper presented a new model for the optimization and visualizing of construction site risk. The model investigates the optimal site layout which minimizes the total risk of facilities. It generates an optimized layout of the construction facilities based on the hazard generated by the potential sources and the vulnerability of the surrounding potential targets. Moreover, it is capable of visualizing a risk due to any potential hazards, within a construction site, through integrating facilities' potential global impact values with mean depth values together utilizing the GIS. In practice, the proposed methodology requires four phases: (1) the creation of interaction matrices; (2) identification of the decision variables, constraints and the objective function for optimization; (3) implementation of space syntax principles and (4) utilization of the GIS for risk mapping of the layout.

For illustrative purposes, a case project layout with various facilities was implemented. It demonstrates that the proposed integrated framework and models for hazard and vulnerability interactions are powerful and useful. It shows the potential global impact of facilities and space configurations effects on the actual risk within a construction site. In addition, the framework provides a risk based optimization of the layout, thus minimizing the areas subjected to risk.

The proposed model creates an optimal layout based on Euclidian distances between facilities. Utilizing the actual distance between them by considering potential barriers and obstacles will provide more accurate data. Furthermore, the facility optimal location can be enhanced by providing additional decision variables like facility rotation. Also, performing specific studies based on the type of hazard provides adequate hazard attenuation with distance. In addition, physical and mechanical sophisticated models can identify adequate conditional vulnerability of facilities and provide more accurate risk variability within a site. Additional future developments of this research are: generating optimal layout based on the amplified risk and finding the optimal path for evacuation in case of emergency.

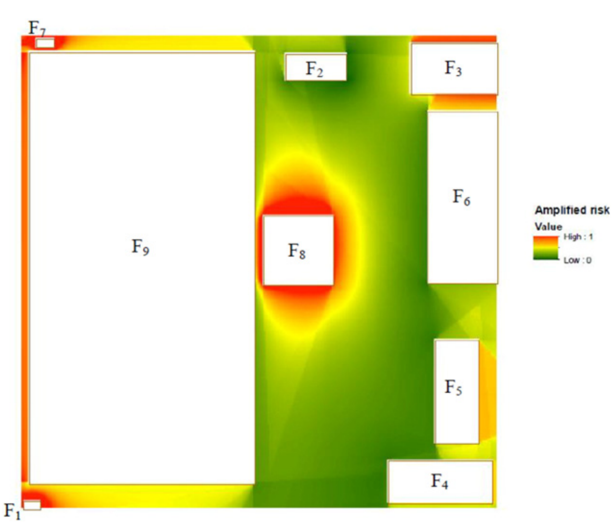

Fig. 11. Map of spatial variability of risk within a site (risk amplification factor ($\mathcal{R}_{af}$)).

Acknowledgments

The authors are grateful to the École Spéciale des Travaux Publics (ESTP) in France and An-Najah National University in Palestine for providing assistance, financial support and the requirements to complete this research. Theoretical developments have also benefited from the Chinese-French program, PHC-CaiYuanpei ("Havu-Risk: Chemical industrial plants & domino effect: hazards, vulnerability, risks & sustainability" 32114TE, 2014–2016).

References

[1] K. El-Rayes, H. Said, Global optimization of dynamic site layout planning in construction projects, Construction Research Congress 2009@ sBuilding a Sustainable Future, ASCE 2009, pp. 846–855.
[2] S. Zolfagharian, J. Irizarry, Current trends in construction site layout planning, Construction Research Congress 2014, pp. 1723–1732.
[3] C. Huang, C.K. Wong, Optimisation of site layout planning for multiple construction stages with safety considerations and requirements, Autom. Constr. 53 (2015) 58–68.
[4] K. El-Rayes, A. Khalafallah, Trade-off between safety and cost in planning construction site layouts, J. Constr. Eng. Manag. 131 (11) (2005) 1186–1195.
[5] H.M. Sanad, M.A. Ammar, M.E. Ibrahim, Optimal construction site layout considering safety and environmental aspects, J. Constr. Eng. Manag. 134 (7) (2008) 536–544.
[6] P.P. Zouein, I.D. Tommelein, Dynamic layout planning using a hybrid incremental solution method, J. Constr. Eng. Manag. 125 (6) (1999) 400–408.
[7] M. Andayesh, F. Sadeghpour, The time dimension in site layout planning, Autom. Constr. 44 (2014) 129–139.
[8] A.D. Patil, D.A. Joshi, A review paper on construction site layout planning, Int. J. Innov. Eng. Technol. (IJIET) 3 (2) (2013).
[9] T. Hegazy, E. Elbeltagi, EvoSite: evolution-based model for site layout planning, J. Comput. Civ. Eng. 13 (3) (1999) 198–206.
[10] P.P. Zouein, H. Harmanani, A. Hajar, Genetic algorithm for solving site layout problem with unequal-size and constrained facilities, J. Comput. Civ. Eng. 16 (2) (2002) 143–151.
[11] H. Said, K. El-Rayes, Performance of global optimization models for dynamic site layout planning of construction projects, Autom. Constr. 36 (2013) 71–78.
[12] M. Andayesh, F. Sadeghpour, Dynamic site layout planning through minimization of total potential energy, Autom. Constr. 31 (2013) 92–102.
[13] M.Y. Cheng, J.T. O'Connor, Site layout of construction temporary facilities using an enhanced-geographic information system (GIS), Autom. Constr. 3 (1) (1994) 11–19.
[14] M.Y. Cheng, J.T. O'Connor, ArcSite: enhanced GIS for construction site layout, J. Constr. Eng. Manag. 122 (4) (1996) 329–336.
[15] A.R. Andoh, X. Su, H. Cai, A framework of RFID and GPS for tracking construction site dynamics, Proc., Construction Research Congress 2012, pp. 818–827.

[16] S. Kang, J. Seo, GIS method for haul road layout planning in large earthmoving projects: framework and analysis, J. Constr. Eng. Manag. 139 (2) (2012) 236–246.
[17] H. Astour, V. Franz, BIM-and simulation-based site layout planning, Computing in Civil and Building Engineering (2014), ASCE 2014, pp. 291–298.
[18] E. Elbeltagi, T.M. Hegazy, Optimum layout planning for irregular construction sites, Proceedings of the 5th CSCE Construction Specialty Conference, Moncton, NB, Canada, COG197, 2003.
[19] D. Dagan, S. Isaac, Planning safe distances between workers on construction sites, Autom. Constr. 50 (2015) 64–71.
[20] A. Mebarki, S. Jerez, I. Matasic, G. Prodhomme, M. Reimeringer, Explosions and structural fragments as industrial hazard: domino effect and risks, Procedia Eng. 45 (2012) 159–166.
[21] A. Mebarki, N. Valencia, J.L. Salagnac, B. Barroca, Flood hazards and masonry constructions: a probabilistic framework for damage, risk and resilience at urban scale, Nat. Hazards Earth Syst. Sci. 12 (5) (2012) 1799–1809.
[22] A. Mebarki, S. Jerez, I. Matasic, G. Prodhomme, M. Reimeringer, V. Pensee, Q.A. Vu, A. Willot, Domino effects and industrial risks: integrated probabilistic framework–case of tsunamis effects, Tsunami Events and Lessons Learned, Springer Netherlands 2014, pp. 271–307.
[23] A. Mebarki, B. Barroca, Resilience and vulnerability analysis for restoration after tsunamis and floods: the case of dwellings and industrial plants, Post-Tsunami Hazard: Reconstruction and Restoration, 44 2014, pp. 237–257.
[24] J. Bin, C. Christophe, K. Bjorn, Integration of space syntax into GIS for modeling urban spaces, Int. J. Appl. Earth Obs. Geoinf. 2 (3r4) (2000) 161–171.
[25] H. Pourvaziri, B. Naderi, A hybrid multi-population genetic algorithm for the dynamic facility layout problem, Appl. Soft Comput. 24 (2014) 457–469.
[26] A.M. El Ansary, M.F. Shalaby, Evolutionary optimization technique for site layout planning, Sustain. Cities Soc. 11 (2014) 48–55.
[27] S.M. Easa, K.M.A. Hossain, New mathematical optimization model for construction site layout, J. Constr. Eng. Manag. 134 (8) (2008) 653–662.
[28] B. Hillier, Space is the machine: a configurational theory of architecture, Space Syntax, London, United Kingdom, Electronic ed.University of Cambridge, 2007.
[29] E.A.L. Teo, F.Y.Y. Ling, A.F.W. Chong, Framework for project managers to manage construction safety, Int. J. Proj. Manag. 23 (4) (2005) 329–341.
[30] C.M. Tam, S.X. Zeng, Z.M. Deng, Identifying elements of poor construction safety management in China, Saf. Sci. 42 (7) (2004) 569–586.
[31] L. Hui, W. Yongqing, S. Shimei, S. Baotie, Study on safety assessment of fire hazard for the construction site, Procedia Eng. 43 (2012) 369–373.
[32] U.S. Fire Administration, Topical Fire Research Series, vol. 2Construction Site Fires, 14 November 2001 (Rev. March 2002).
[33] K.C. Lam, X. Ning, M.C.K. Lam, Conjoining MMAS to GA to solve construction site layout planning problem, J. Constr. Eng. Manag. 135 (10) (2009) 1049–1057.
[34] A. Kusiak, S.S. Heragu, The facility layout problem, Eur. J. Oper. Res. 29 (3) (1987) 229–251.
[35] S.S. Heragu, A. Kusiak, Efficient models for the facility layout problem, Eur. J. Oper. Res. 53 (1) (1991) 1–13.
[36] M.E.H. Pedersen, Good Parameters for Differential Evolution, Magnus Erik Hvass Pedersen, 2010.
[37] R. Storn, K. Price, Differential evolution–a simple and efficient heuristic for global optimization over continuous spaces, J. Glob. Optim. 11 (4) (1997) 341–359.
[38] E. Mezura-Montes, M.E. Miranda-Varela, R. del Carmen Gómez-Ramón, Differential evolution in constrained numerical optimization: an empirical study, Inf. Sci. 180 (22) (2010) 4223–4262.